AlInGaAs/AlGaAs Strained Quantum Well Lasers Grown by Molecular Beam Epitaxy

Yang Guowen(杨国文), Xu Zuntu(徐遵图), Xu Junying(徐俊英),

Zhang Jingming(张敬明), Xiao Jianwei(肖建伟) and Chen Lianghui(陈良惠)

(*Institute of Semiconductors, The Chinese Academy of Sciences, Beijing* 100083)

Abstract   AlInGaAs/AlGaAs strained single quantum well lasers with an emission wavelength of 810nm were fabricated by molecular beam epitaxy(MBE). The threshold current density is 375A/cm² for broad-area lasers(100×800μm²), and it decreases to 270A/cm² when the cavity length extends to 1600μm, which is the best result in quaternary AlInGaAs/AlGaAs strained quantum well lasers for the as-grown wafer by MBE. An external differential quantum efficiency of 1. 1W/A(72%) and a narrow transverse beam divergence of 34° are obtained for the uncoated lasers.

PACC: 4255P, 6855, 7360F, 8115N

1　Introduction

Strained InGaAs/AlGaAs quantum well lasers have demonstrated improved performance compared with lattice-matched, unstrained GaAs/AlGaAs or AlGaAs/AlGaAs quantum well lasers[1,2], which has been attributed to modifications of the band structure due to the strained nature of InGaAs layer[3]. In addition, a significant advantage of the improvement in laser reliability has been demonstrated[4~6]. In order to take advantage of the benefits ascribed to In incorporation and extend the wavelength to other useful range, aluminum can be incorporated into InGaAs quantum well structures. By the addition of Al, the bandgap energy will be increased, thereby reducing the emission wavelength. The resulting quaternary AlInGaAs strained quantum well lasers can operate over a very wide range of wavelengths depending on the In and Al composition[7]. So far, most of the AlInGaAs/AlGaAs quantum well lasers have been grown by metal-organic chemical vapor deposition(MOCVD)[7~10], but few of them have been grown by solid-source molecular beam epitaxy(MBE)[11]. In this letter, we report an AlInGaAs/AlGaAs quantum well laser emitting at 810nm with a record threshold current density of 270A/cm² for the as-grown wafer by MBE. The uncoated broad-area lasers(100×800μm²), which exhibit an external

differential quantum efficiency of 1. 1W/A(72%), and a narrow transverse beam divergence of 34°, represent the high performance of lasers using this new combination of materials grown by MBE.

2　Laser structure and fabrication

The critical thickness of AlInGaAs layer in strained AlInGaAs/AlGaAs quantum well lasers is the same as that of InGaAs layer in InGaAs/AlGaAs lasers. For In composition of 0. 15, the lattice mismatch is about 1. 1%, and the critical thickness is about 20nm.

The laser structure was grown in a RIBER MBE 32P system on a 3° off (100) towards $\langle 111 \rangle$A n^+-GaAs substrate. Arsenic source is As_4, and the n and p dopants are Si and Be, respectively. The graded-index separate confinement heterostructure(GRIN-SCH) single quantum well(SQW) laser consists of the following layers: 300nm of n^+-GaAs buffer-layer doped $2 \times 10^{18} cm^{-3}$, 100nm of linearly graded n-$Al_{0.1 \sim 0.5}Ga_{0.9 \sim 0.5}$As layer doped 2×10^{18} cm^{-3}, 1. 5μm of n-$Al_{0.5}Ga_{0.5}$As as the lower cladding layer doped $1 \times 10^{18} cm^{-3}$, 70nm of undoped linearly graded $Al_{0.5 \sim 0.3}Ga_{0.5 \sim 0.7}$As lower waveguide layer, a 8. 5nm $Al_{0.15}In_{0.15}$ $Ga_{0.7}$As quantum well sandwiched by 25nm of $Al_{0.3}Ga_{0.7}$As barrier layer, 70nm of undoped linearly graded $Al_{0.3 \sim 0.5}Ga_{0.7 \sim 0.5}$As upper waveguide layer, 1. 5μm of p-$Al_{0.5}Ga_{0.5}$As as the upper cladding layer doped $1 \times 10^{18} cm^{-3}$, 100nm of linearly graded p-$Al_{0.5 \sim 0.1}Ga_{0.5 \sim 0.9}$As layer doped $2 \times 10^{18} cm^{-3}$, 150nm of p^+-GaAs doped $1 \times 10^{19} cm^{-3}$, and 20nm of p^+-GaAs ohmic-contact layer doped $5 \times 10^{19} cm^{-3}$.

During the MBE growth, all the AlGaAs layers, except barrier and active layers, were grown at a constant temperature of 700℃, the n^+-GaAs buffer layer and p^+-GaAs layer were grown at 600℃, and the active layer was grown at 580℃. The temperature was ramped from 700℃ to 580℃ or vice-versa during the growth of $Al_{0.3}Ga_{0.7}$As barrier layer. No growth interruption was used during the growth. V / Ⅲ flux ratio was selected near-critical arsenic-stabilized condition, and the growth rate for GaAs was 0. 8μm/h.

After growth, a conformal 120nm-thick SiO_2 was deposited over the entire p-surface by Plasma-Enhanced Chemical Vapor Deposition(PECVD), then the wafer was processed into wide-stripe(100μm) lasers using standard photolithography techniques. After the p-contact consisting of Ti/Pt/Au was deposited, the wafer was thinned to a thickness of about 100μm, then the n-contact consisting of AuGe/Ni/Au was deposited. The lasers were then cleaved into uncoated bars of intended various cavity lengths. The tested devices were mounted p-side down on a copper heat-sink by using indium solder.

Fig. 1　Threshold current density J_{th} of AlInGaAs/AlGaAs strained quantum well lasers as a function of cavity length L

3　Experimental Results

Fig. 1 shows the plot of threshold current density (J_{th}) against various cavity lengths L for the fabricated lasers. The threshold current density is
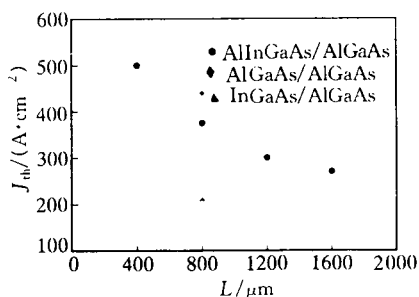
375A/cm² at cavity length of 800μm, and this value takes no account of any current spreading, nor of the anti-guiding effects which widen the effective stripe width. When the cavity length extends to 1600μm, the threshold current density (J_{th}) is 270A/cm². In Fig. 1, we also give the typical J_{th} value for our fabricated AlGaAs/AlGaAs and InGaAs/AlGaAs quantum well lasers. Because the three structures are similar, we believe that the lower J_{th} values of the AlInGaAs/AlGaAs lasers in comparison to the AlGaAs/AlGaAs devices show the basic advantage of the quaternary material, which can be expected because the biaxial compressive strain reduces the valence band density of states, and should there-

fore decrease the current density needed for population inversion. The AlInGaAs/AlGaAs lasers have higher J_{th} value than the InGaAs/AlGaAs devices, possibly because the addition of Al in the active layer increases both the conduction and valence band effective mass.

In Fig. 2, the reciprocal of η_d is plotted *vs* L for the AlInGaAs/AlGaAs GRIN-SCH-SQW lasers. The value of η_d increases from 59% for L =1600μm to 80% for L=400μm. From the intercept and slope, the internal quantum effiency η_i and total internal loss α_i are found to be 0.91 and 4cm⁻¹, respectively. These values are typical of

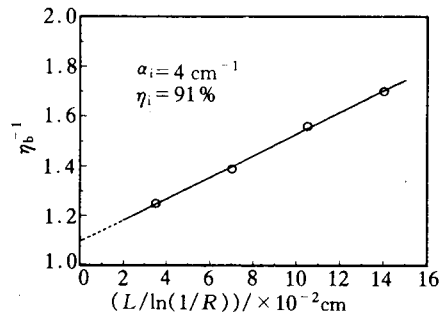Fig. 2 Reciprocal differential quantum efficiency η_d^{-1} as a function of cavity length L/ln $(1/R)$ for AlInGaAs/AlGaAs diode lasers

our InGaAs/AlGaAs lasers and better than our AlGaAs/AlGaAs lasers.

For an uncoated wide stripe (100μm) AlInGaAs/AlGaAs strained quantum well laser having a cavity length of 800μm, the light output versus CW drive current characteristics to an output power level of 600mW is shown in Fig. 3, which was measured from an uncoated 100μm-wide stripe laser having a cavity length of 800μm. The threshold current is 300mA and the operating current at 600mW is 1.38A, so an external quantum efficiency of 0.55W/A (36%) per facet could be deduced. In Fig. 3, the operating voltage as a function of driving current is also demonstrated, and the differential resistance is 0.2Ω. The inset presents the emission spectrum measured at a CW output of 300mW.
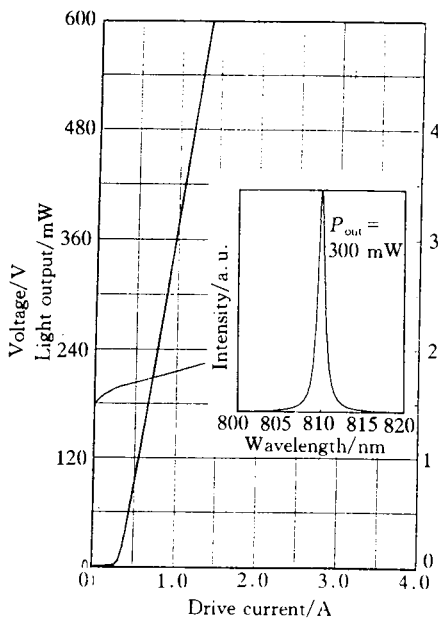

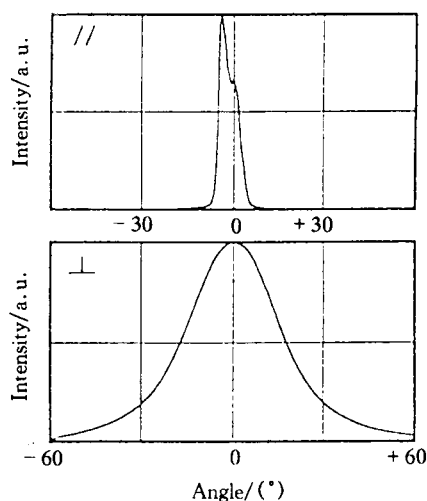Fig. 3 CW output power and forward voltage against driving current

Fig. 4 shows both the parallel and perpendicular far-field intensity profiles corresponding to CW output power of 300mW per facet. The parallel far-field angle at full width half maximum (FWHM) is 7°. The perpendicular far-field angle at FWHM is 34°. The narrow perpendicular beam divergence is attributed to the weak optical confinement in our laser structure. This is very useful for the device applications in systems so that efficient fiber coupling or high pumping efficiency can be achieved. If strong optical confinement in the laser structure is used, the threshold current density will decrease more.

Fig. 4　Parallel and perpendicular far-field intensity profiles of an AlInGaAs/AlGaAs wide stripe laser device

4　Conclusion

In this paper, we have shown that it is possible to achieve high performance strained AlInGaAs/AlGaAs quantum well lasers for the as-grown wafer by solid source MBE. We have also demonstrated that the performance of strained AlInGaAs/AlGaAs quantum well lasers is improved over AlGaAs/AlGaAs lasers. For a 8.5nm-thick $Al_{0.15}In_{0.15}Ga_{0.7}As$ quantum well active layer, the lasing wavelength is 810nm. A record low CW threshold current density of $270A/cm^2$ in wide stripe lasers for $L=1600\mu m$ is obtained. An internal quantum efficiency as high as 91%, a low internal loss of $\alpha_i=4cm_{-1}$, and a narrow transverse beam divergence of 34° are measured.

References

[1]　N. Chand, E. E. Becker, Van Der Ziel et al. , Appl. Phys. Lett. , 1991, **58**: 1704~1706.

[2]　H. K. Choi and C. A. Wang, Appl. Phys. Lett. , 1990, **57**: 321~323.

[3]　E. P. O'Reilly and A. R. Adams, IEEE J. Quantum Electron. , 1994, **30**: 366~379.

[4]　S. E. Fischer, R. G. Waters, D. Fekete et al. , Appl. Phys. Lett. , 1989, **54**: 1861~1862.

[5]　D. P. Bour, D. B. Gilbert, K. B. Fabian et al. , IEEE Photon. Technol. Lett. , 1990, **2**: 173~174.

[6]　R. G. Waters, D. P. Bour, S. L. Yellen et al. , IEEE Photon. Technol. Lett. , 1990, **2**: 531~533.

[7]　C. A. Wang, J. N. Walpole, L. J. Missaggia et al. , Appl. Phys. Lett. , 1991, **58**: 2208~2210.

[8]　C. A. Wang, J. N. Walpole, H. K. Choi et al. , IEEE Photon. Technol. Lett. , 1991, **3**: 4~5.

[9]　L. Buydens, P. Demeester, M. Van Ackere et al. , Electron. Lett. , 1991, **27**: 618~620.

[10]　J. Baumann, S. Yellen, R. Juhala et al. , SPIE, Laser Diode Technology and Applications V, 1993, **1850**: 203~214.

[11]　J. Ko, M. J. Mondry, D. B. Young et al. , Electron. Lett. , 1996, **32**: 351~352.